

Some results of PMT studies

LHCB Technical Note

Issue: Draft
Revision: 2

Reference: LHCB 2000-52
Created: 15- August 2000
Last modified:

Prepared By: R CIZERON, J-M NOPPE, B. JEAN-MARIE, K. TRUONG

Laboratoire de l'Accélérateur Linéaire (LAL) ORSAY FRANCE

Abstract

This note reports on the preliminary testing of presently available commercial PMTs to equip the LHCB calorimeters. Among the many characteristics which have to be tested, mainly five have been looked at in this first round of tests: linearity, pulse shape, transit time spread, cathode uniformity and magnetic immunity.

Document Status Sheet

Table 1 Document Status Sheet

1. Document Title: Some results of PMT studies			
2. Document Reference Number: LHCB 2000-52			
3. Issue	4. Revision	5. Date	6. Reason for change
Draft	1	15 August 00	First version

Table of contents

1 Introduction.....	2
2 PMT test Bench.....	3
2.1 Description.....	3
2.1.1 Optical system.....	5
2.1.2 Mechanical support.....	6
2.1.3 Pulse measurement.....	6
2.1.4 Acquisition and control.....	6
2.2 PMT tested.....	7
2.3 Results.....	7
2.3.1 Linearity.....	7
2.3.2 Gain and Pulse parameters.....	10
2.3.3 Cathode response uniformity.....	14
3 Magnetic shielding study.....	17
3.1 Magnetic measurement set-up.....	17
3.2 Results for one shielding tube.....	17
3.3 Results with an array of nine shielding tubes.....	19
3.4 Conclusions for magnetic studies.....	20
4 Conclusions.....	21
5 References.....	22

1 Introduction

The LHCb calorimeter system [1] incorporates four different detectors: a Scintillation Pad Detector, a Preshower, an electromagnetic calorimeter (ECAL) and a Hadronic Calorimeter (HCAL).

The ECAL is based on a Shashlik design whereas the HCAL is a scintillating tile calorimeter. Both will be read via wavelength shifting fibres connected at total to about 6000 identical Photo Multiplier Tubes (PMT). As far as PMTs are concerned, the main difference between the two calorimeters comes from the photon yield that is 50 photoelectrons per GeV for HCAL against 1000 for ECAL. The electronics, which will equip both calorimeters, tolerates a maximum current of about 20 mA into 50Ω . Thus, the same PMT will have to work at gain ranging from 10^4 to 10^6 .

2 PMT test Bench

2.1 Description

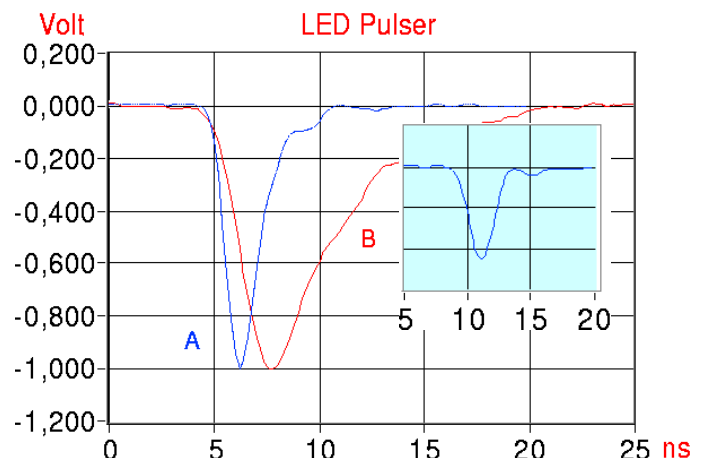
A dedicated test bench [2] has been built to perform the following measurements: gain, linearity, transit time measurements versus voltage, photo cathode scan and stability measurements over days. With the present setup, it is possible to vary automatically high voltages, to drive and control a variable pulsed light source and to record pulse amplitudes or integrals.



Figure 2-1

The main mechanical and optical components of the test bench are seen in Fig. 2-3. Very short light pulses (Fig. 2-2) are obtained by driving a blue LED emitting diode using a mercury relay. The repetition rate is 50 Hz. The voltage applied is programmable between 20 and 200 volts resulting in a factor 5 variation in light yield. (Fig. 2-4)

Figure 2-2 A) Driving pulse generated by a mercury relay. Risetime=1ns. B) Light pulse emitted by the diode. Risetime = 2ns. This measurement was done using filters to strongly attenuate the light pulse in order to detect only single photons. The pulse shown is the averaged distribution of 1000 single photons convoluted to the PMT response to one photon shown in the box.



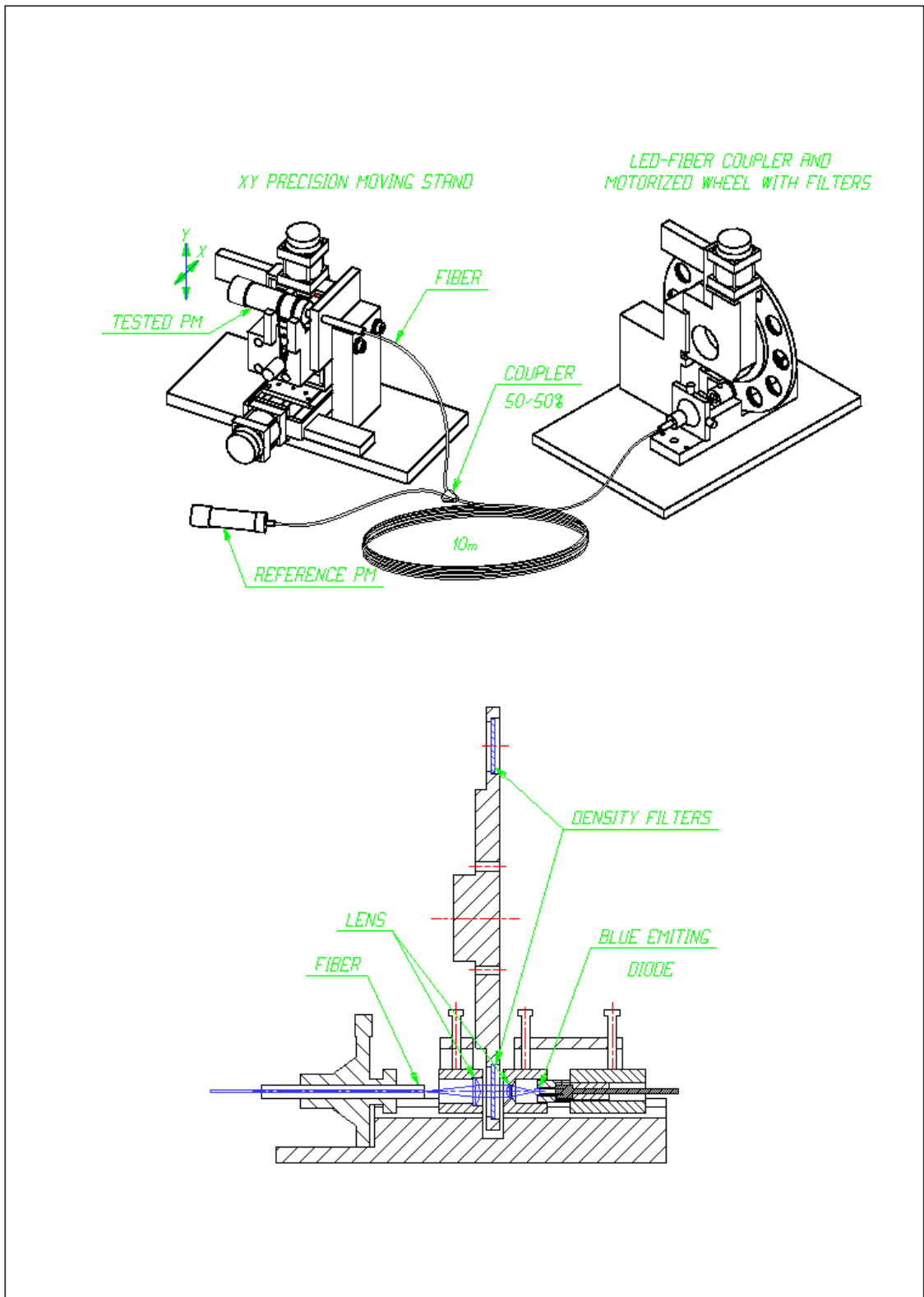


Figure 2-3 Main mechanical and optical components of the test bench

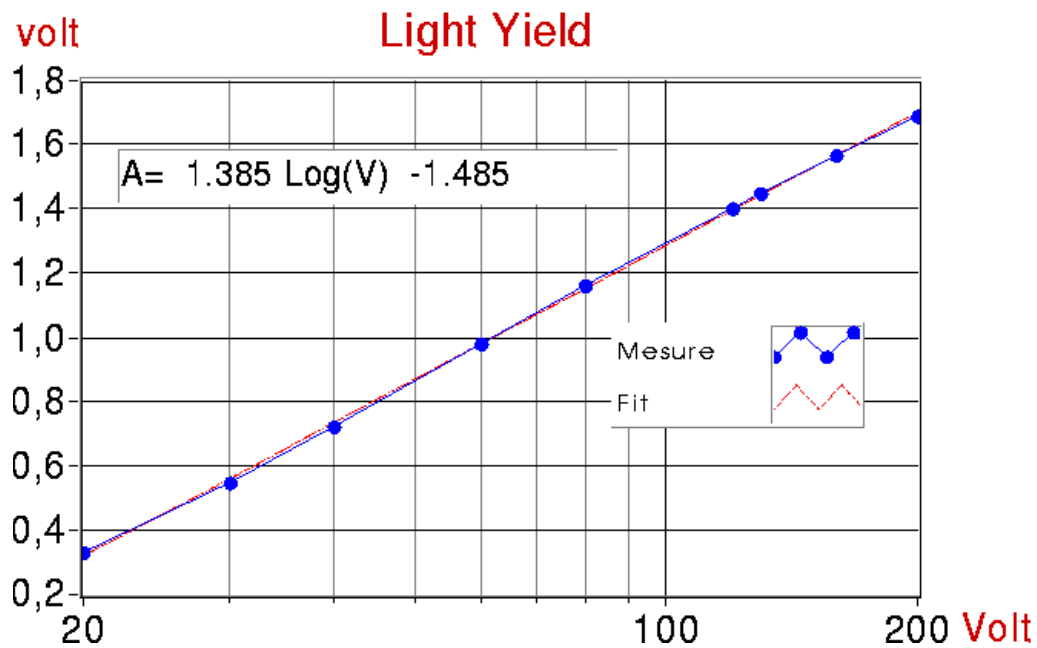


Figure 2-4 Pulse amplitude versus the applied voltage.

2.1.1 Optical system

Light from a photodiode is focussed, through two plano-convex lenses, onto a 200 μm quartz fibre. Between the two lenses a set of eleven neutral density filters are placed on a rotating wheel. A twelfth position has no filter. By positioning the wheel in between filters, one gets a “black filter” position, which is used to record background noise generated by the pulser. The largest attenuation factor is 30. After 9 meters, the fibre is divided in two by a 50/50 optical coupler. The light emission cone angle is 17 degrees (FWHM). The whole system is protected against ambient light.

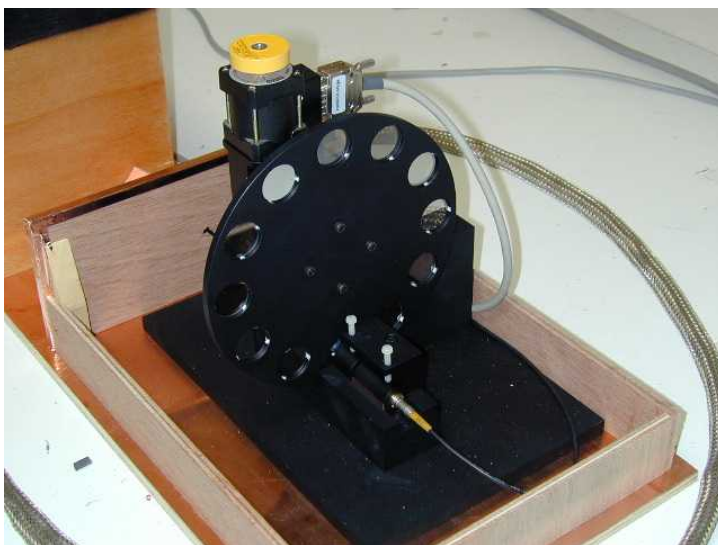


Figure 2-5

2.1.2 Mechanical support

Two PMTs are placed inside a common light-tight box (Fig2-6). One is used as reference (REF) and the other is the PMT being tested. In order to avoid possible light variation when moving a fibre, we have chosen to keep the fibre still and to move the PMT. The PMT under test is mounted on an X-Y moving table allowing precise photocathode scan within ± 2.5 cm. The reproducibility in positioning is better than 100 μm . The table and the filter wheel are remotely controlled.



Figure 2-6 View of the PMT under test fixed on the moving table and the reference PMT on the left

2.1.3 Pulse measurement

PMT signals are analysed by a 500MHz Tektronix TDS3052 digital oscilloscope used as a smart ADC. Digitised pulses (5 samples per nanosecond) are either transferred to a PC or, taking advantage of the computing capability of the scope, are averaged over at most 512 pulses and then recorded. Furthermore, for linearity measurement it is possible to adjust automatically the oscilloscope amplitude scale to get the best possible accuracy.

2.1.4 Acquisition and control

A PC running LabVIEW under Windows NT executes acquisition and control. It is equipped with three specialised cards:

1. A stepper motor controller card MICOS SMC-PC 7190-9-022 programmable via an RS-232 interface.
2. A National Instrument PCI-GPIB card to communicate both to the oscilloscope and to a CAMAC crate containing all the dedicated electronics: HV, pulser, etc.
3. A National Instrument 6023E low cost multifunction 12-bit input/output acquisition card used to survey parameters like temperature, voltages, pulser state etc.

2.2 PMT tested

PMTs from four companies have been considered. Their relevant technical data characteristics for this study are listed in Table 1

	unit	ETL	PHOTONIS				FEU		HAMAMATSU		
		9112B	XP1981	XP2802	XP2961	115M	115M-10	R1924NT	R5800	R7899-01	
Length	mm	43	88	60	60	90	72	43	70	62	
Tube diameter	mm	25	19	19	29	30	30	25	25	25	
Useful photocathode diameter	mm	21	15	15	24	24	24	21	21	21	
Photocathode shape		concave	concave	flat	concave	flat	flat	concave	concave	concave	
Number of dynodes		10	8	10	12	12	10	10	10	10	
Dynode structure		circular	linear	linear	circular	linear	linear	circular	linear	linear	
Gain at nominal voltage		10^5	$2 \cdot 10^5$	$9 \cdot 10^5$	$2 \cdot 10^5$	$0.6 \cdot 10^6$	10^6	$3 \cdot 10^5$	10^6	$5 \cdot 10^5$	
Nominal voltage	volt	1000	1500	1100	1500	1980	1980	1000	1500	1500	
Max voltage	volt	1300	1800	1700	1700	2500	2500				
Anode pulse rise time	ns	2	2	2.2	1.8			1.5	1.5	1.6	
Transit time	ns	20	18	21	20			15	21	17	
Transit time spread	ns							1.9	0.9	0.6	
Max anode current for a linearity better than $\pm 2\%$	mA		80		80	>50		50	100	100	

Table 1

2.3 Results

2.3.1 Linearity

The linearity measurements are done by attenuating the input light pulse and comparing amplitude ratio of the PMT under test and a reference PMT. A PMT FEU115M, 12 stages is used as reference. It is operated at a gain less than 10^5 for which it has a good linearity. Results for the FEU115M -10 are shown in Fig. 2-7. The upper left graph displays the amplitude evolution of the PMT tested versus the REF one with a superimposed fit in red. The deviation from linearity is shown in the upper right graph. The third one shows the linearity evolution calculated from the theoretically known filter densities values and normalised to the first measurement. It gives an independent crosscheck of the linearity. These results agree with those reported in an another Calorimeter LHCb Technical note [3].

A linearity better than $\pm 1\%$ up to 40 mA has been taken as PMT selection criteria. Only three tubes satisfy this requirement: FEU115M-10, R5800, and R7889-01 as shown in Fig. 2-7, 2-8, 2-9. A fourth one (Fig. 2-10), XP2802 tested at rather low gain did not satisfy the criteria. However, this tube being still under development, improvements in future are foreseen.

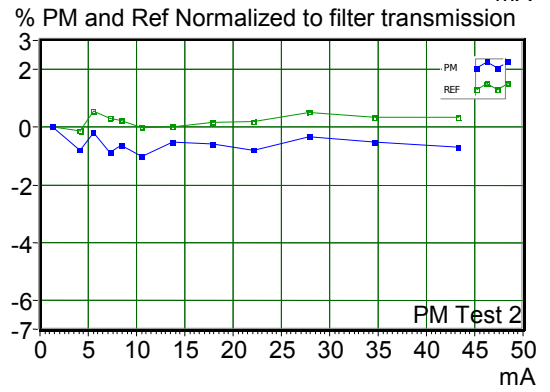
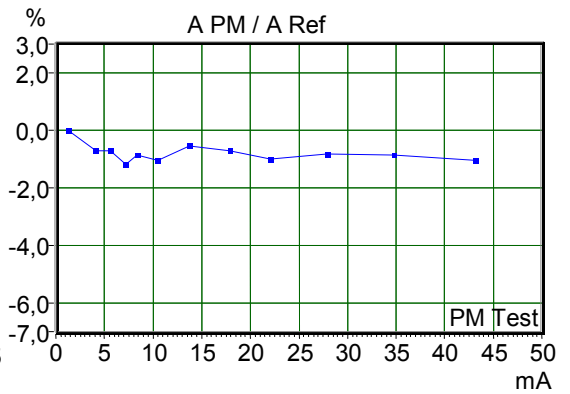
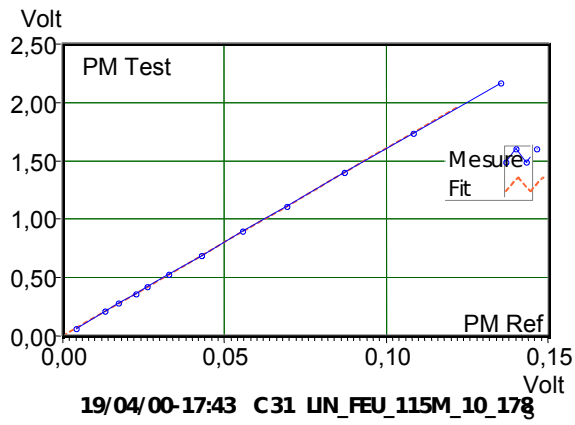


Figure 2-7 Linearity curve for FEU 115M-10 at 1700 volt, HV REF: 1200 volts

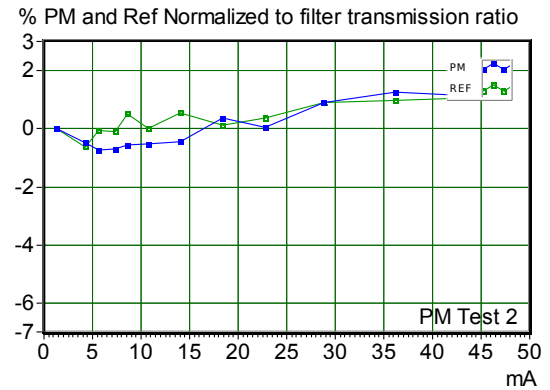
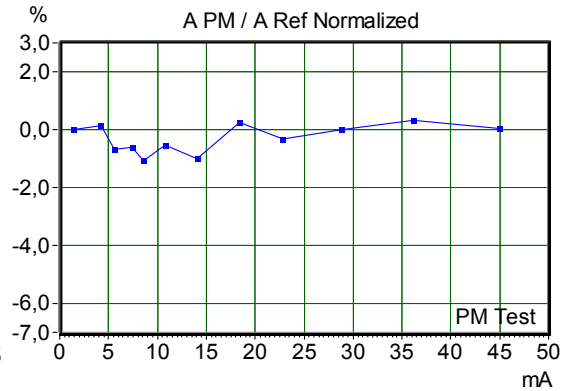
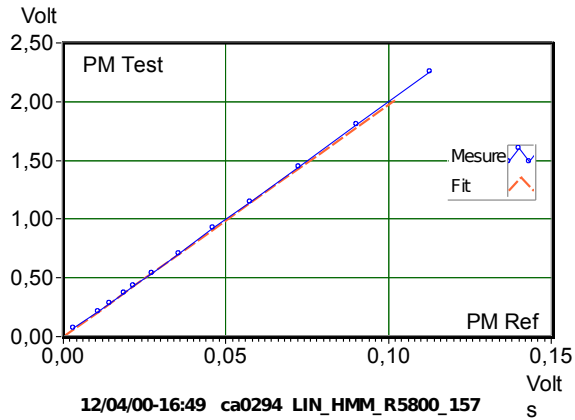


Figure 2-8 Linearity curve for Hamamatsu R5800 at 900 volts. HV REF 1250 volts.

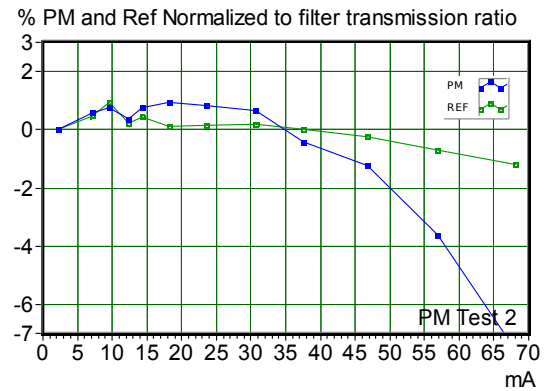
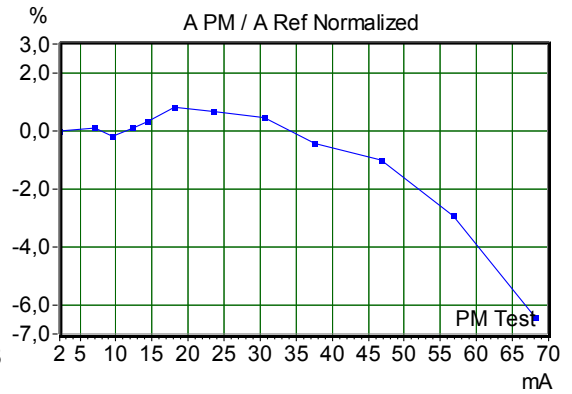
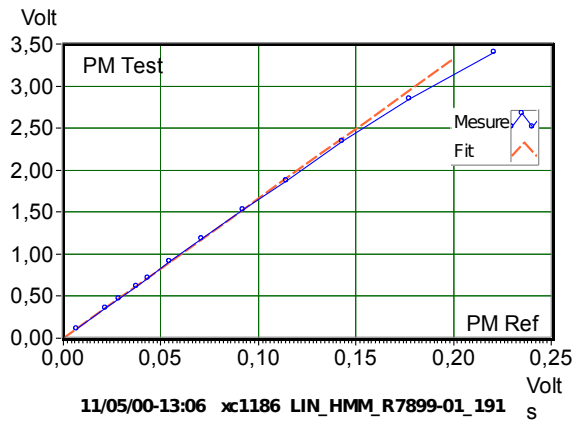


Figure 2-9 Linearity curve for Hamamatsu R7899 at 1100 volts. HV REF 1350 volts.

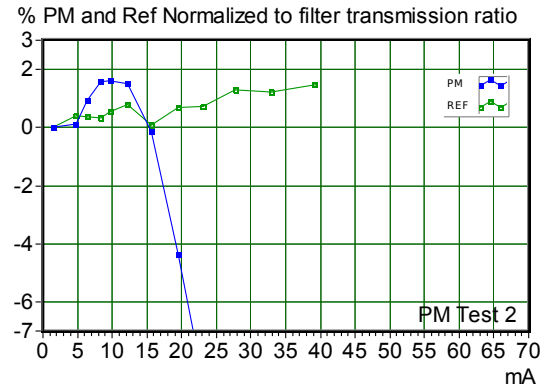
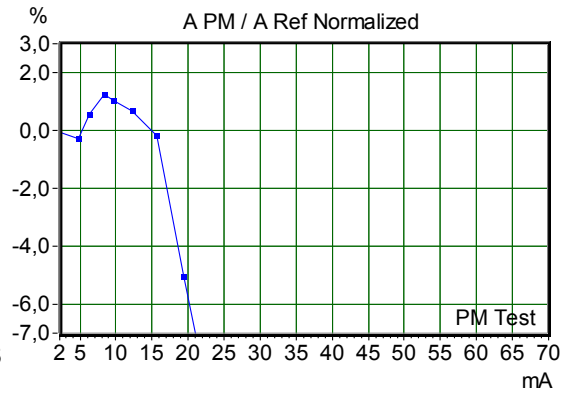
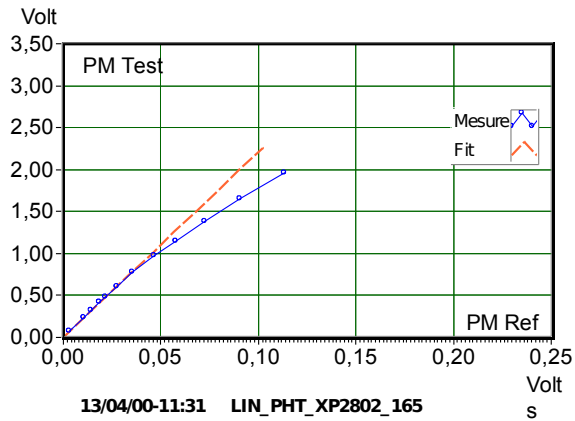


Figure 2-10 Linearity curve for Photonis at 1025 volts. HV REF 1250 volts.

2.3.2 Gain and Pulse parameters

These measurements are done by varying the PM voltage and calculating an averaged pulse for each setting. Then the pulse is processed by a LabVIEW routine. It estimates all the pulse parameters namely the maximum amplitude, the rise-time defined as the time to go from 10% to 90% of the pulse, the transit time taken as the time difference between the trigger and the time at half the maximum amplitude and the fall-time. It has been checked (Fig.2-11) by keeping the same voltage and varying the light intensity, that the routine outputs were not depending upon the amplitude of the input pulse.

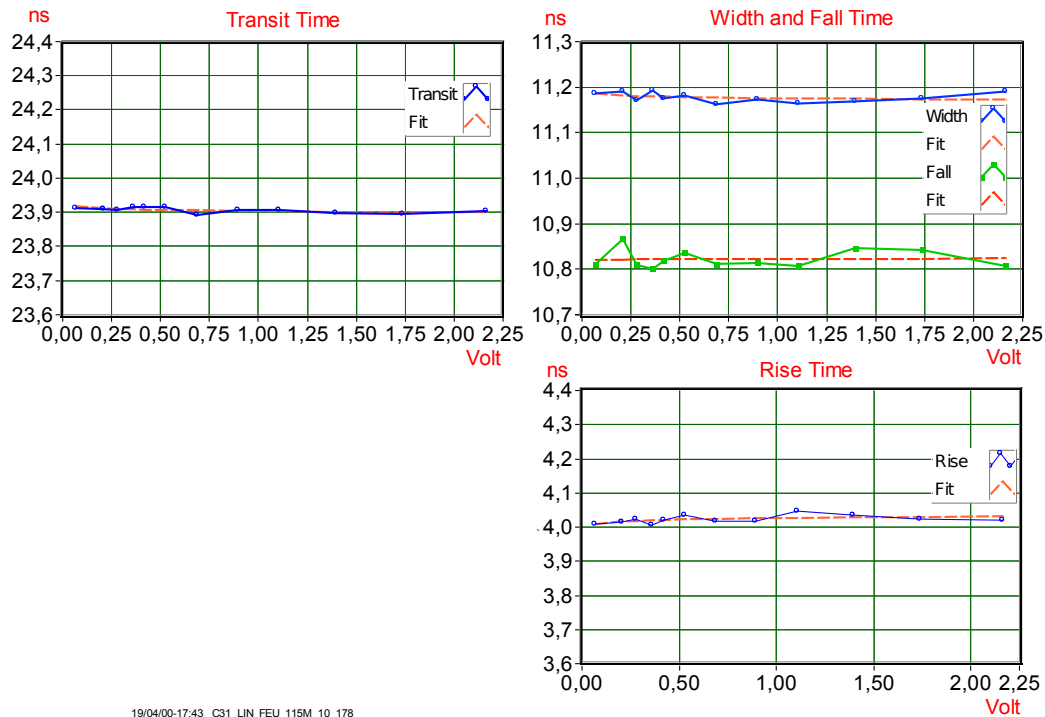


Figure 2-11 Stability of the parameter evaluation

The gain curves are parameterised as $A=kV^n$ and as expected the transit time varies approximately like $1/\sqrt{V}$. Fig. 2-12, 2-13, 2-14, 2-15 show the results.

It is known that among a production of tubes, the gain can vary by more than a factor 10. However, for all three tubes tested, the timing variations, within that gain factor, still stay within a few nanoseconds and can be easily corrected by the foreseen electronics.

As shown Fig. 2-16 and table 2, the pulses from Hamamatsu tubes are substantially faster and shorter than for the FEU one. However, in any case, the pulse will be broadened due to the scintillation decay time and the fibre time response. Furthermore, the electronics is designed to clip the pulse in order to shorten it to no more than 25ns.

	Rise time	Width	Fall time	Total
	ns	ns	ns	ns
FEU 115M-10	4.15	11.7	11.3	27.1
Hamamatsu R5800	3.1	7.5	10	20.6
Hamamatsu R7899-01	2.9	6.4	9.1	18.4

Tableau 2 Pulse comparison.

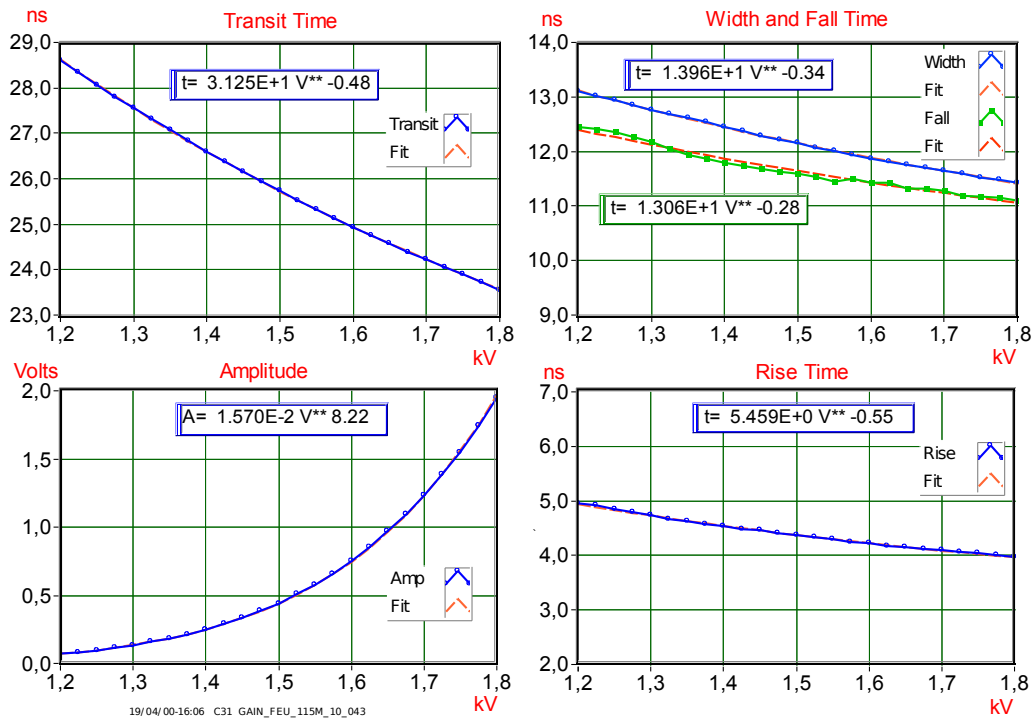


Figure 2-12 Gain and pulse parameters for FEU115M-10

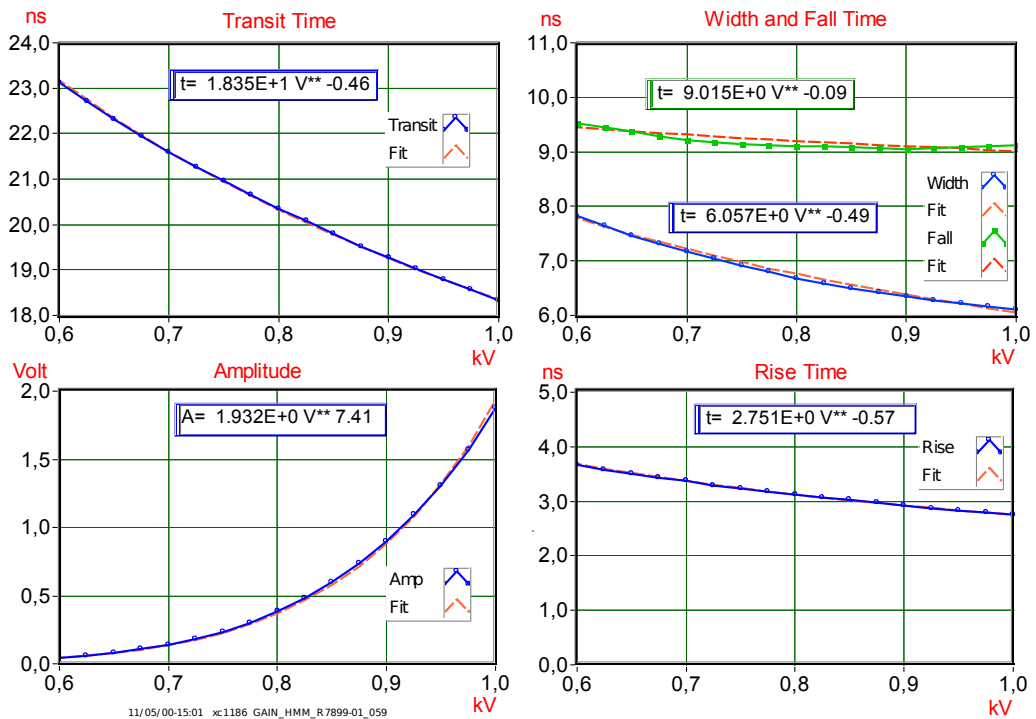


Figure 2-13 Gain and pulse parameters for Hamamatsu R7899-01

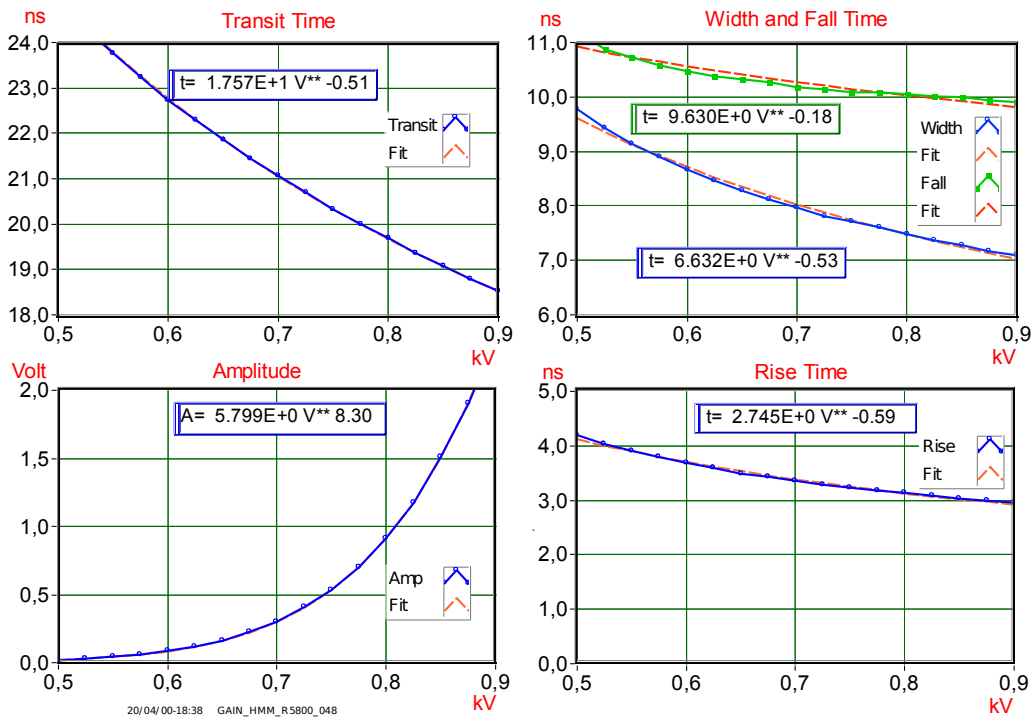


Figure2-14 Gain and Pulse parameters for Hamamatsu R5800.

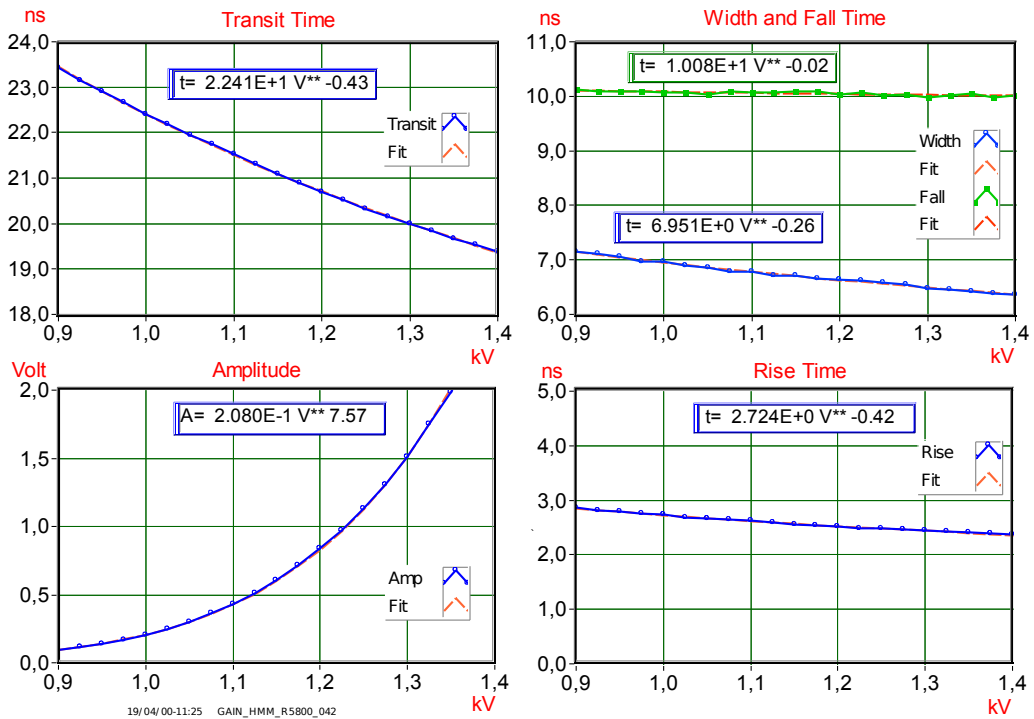


Figure 2-15 Gain and pulse parameters for Hamamatsu R5800.

Arbitrary Scale

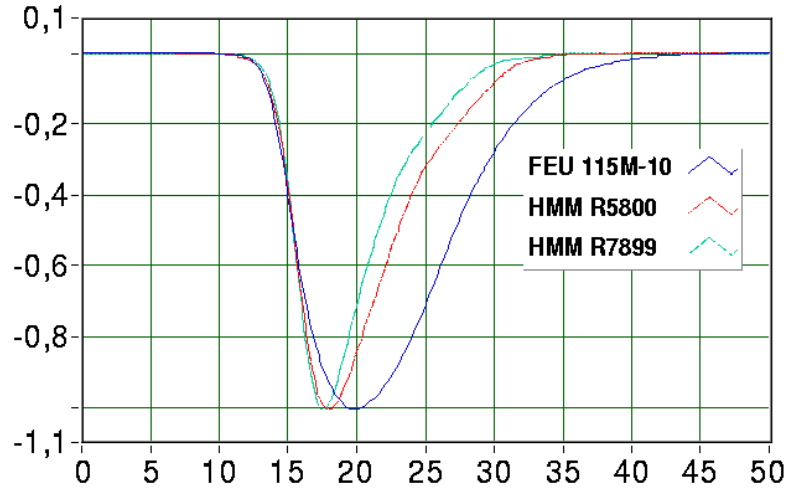


Figure 2-16 Pulse comparison for the three tubes at approximately the same gain.

Table 3 summarise the PMT properties for the three tubes passing the linearity criteria.

		FEU 115M-10	Hamamatsu R5800	Hamamatsu R7899-01
Length	mm	72	70	62
Tube diameter	mm	30	25	25
Useful photocathode diameter	mm	24	21	21
Gain V^{α}	-	8.22	8.30	7.22
X2 increase gain	volt	130	90	70
X10 increase gain	volt	440	340	260
Linearity+1%	ma	>50	>50	40
Transit time	ns	24.5	19.5	19
Δt transit time	ns	8	-	0.6
Δt transit time within 1cm ²	ns	1	-	0.25
Cathode non-uniformity	%	50	50	16
Cathode non-uniformity within 1 cm ²	%	30	30	8
Total pulse spread	ns	27.1	19.6	18.4

Tableau 3 Summary of PMT properties.

2.3.3 Cathode response uniformity

Scans of photocathode surface were done in X and Y steps of 1mm, the fibre being located at 1mm from the photocathode window. Both the amplitude and the transit time were recorded. The signal from the reference PMT was used to control the stability of the diode light pulse. The response map obtained combines photocathode non-uniformity and possible anomalies in the dynode amplification chain.

Large non-uniformities in amplitude are observed in scanning FEU115M-10 (Fig. 2-17) and Hamamatsu R5800 (Fig. 2-18). However the Hamamatsu R7899-01 (Fig. 2-19) is uniform. The non-uniformity in amplitude comes mainly from an imperfect photocathode deposition. This problem, which depends only of the manufacturing process, may certainly be corrected.

In comparison, the transit time spread depends mostly upon the tube structure and varies little from tube to tube. The variations measured are smooth. The Hamamatsu R7899-01 (Fig. 2-20) has a remarkably small transit time spread of less than one nanosecond for the whole surface. However, due to the foreseen use of a light mixer between the PMT and the fibre bundle, the non-uniformity in time (or amplitude) is only important within a 1cm squared surface near the photocathode centre. With that restriction, the FEU transit time spread (Fig. 2-21) has an acceptable value of about 1ns.

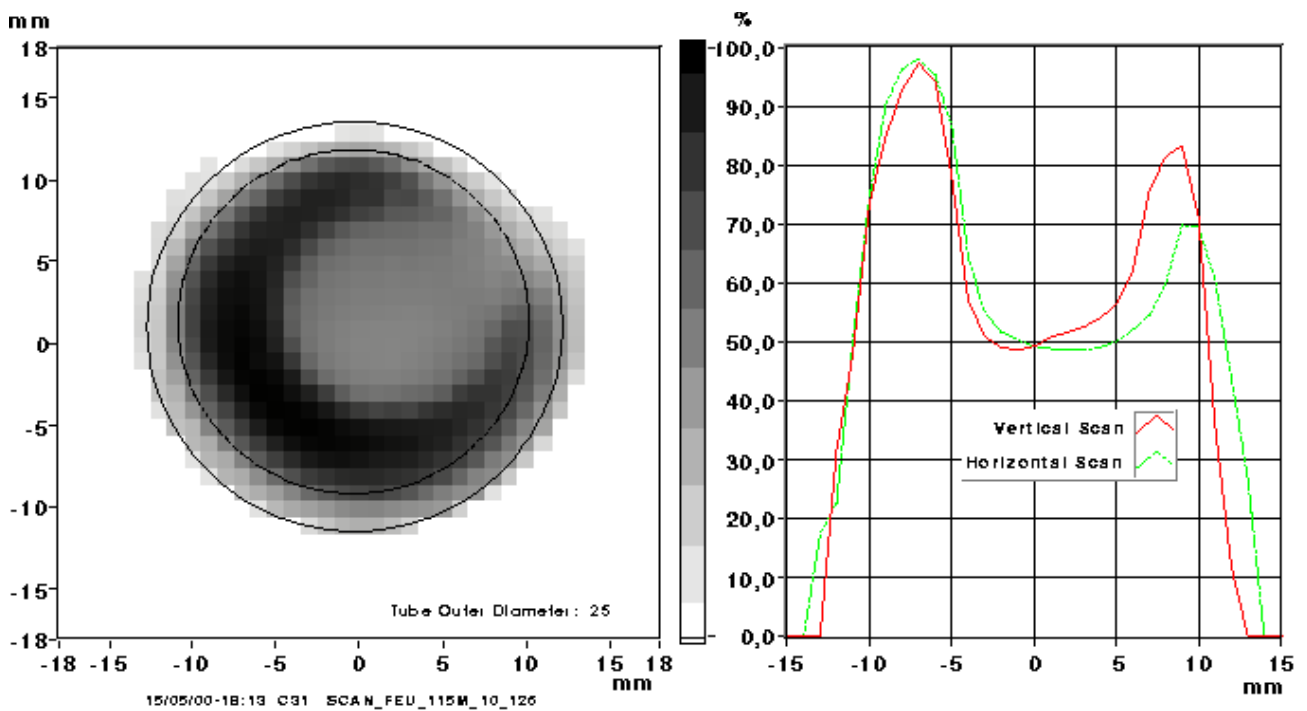


Figure 2-17

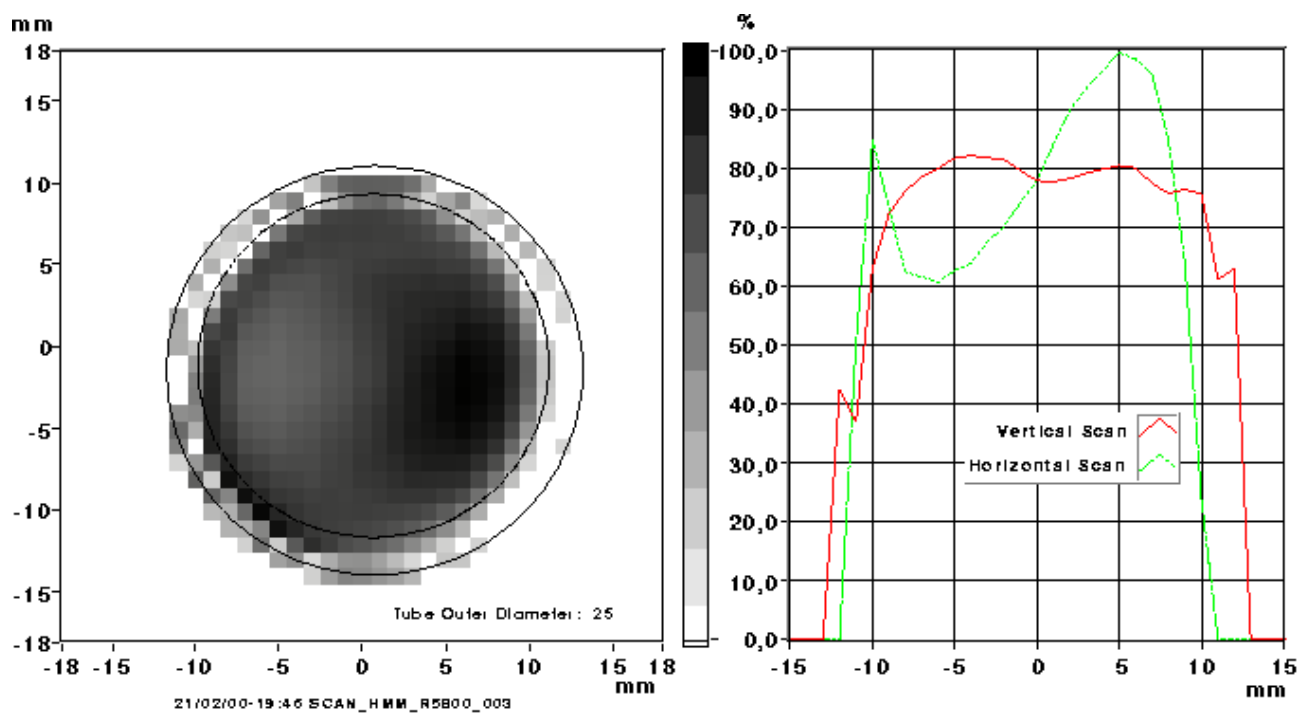


Figure 2-18

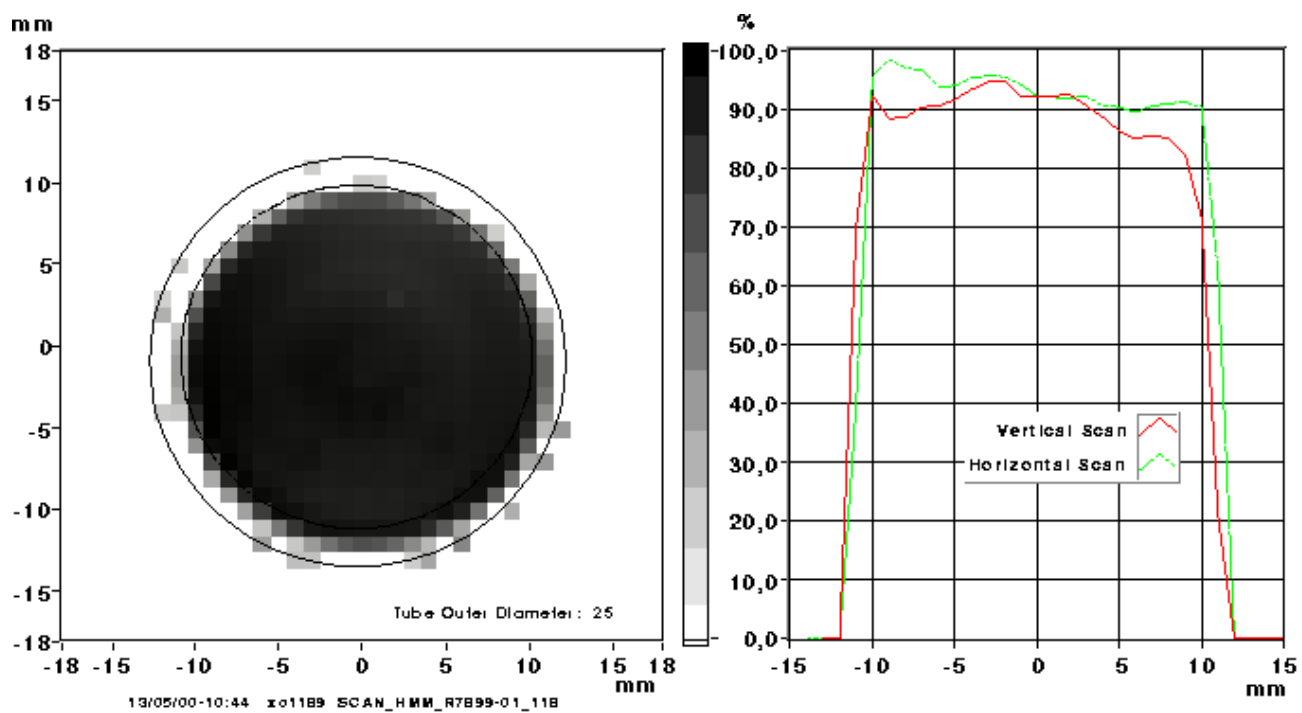


Figure 2-19

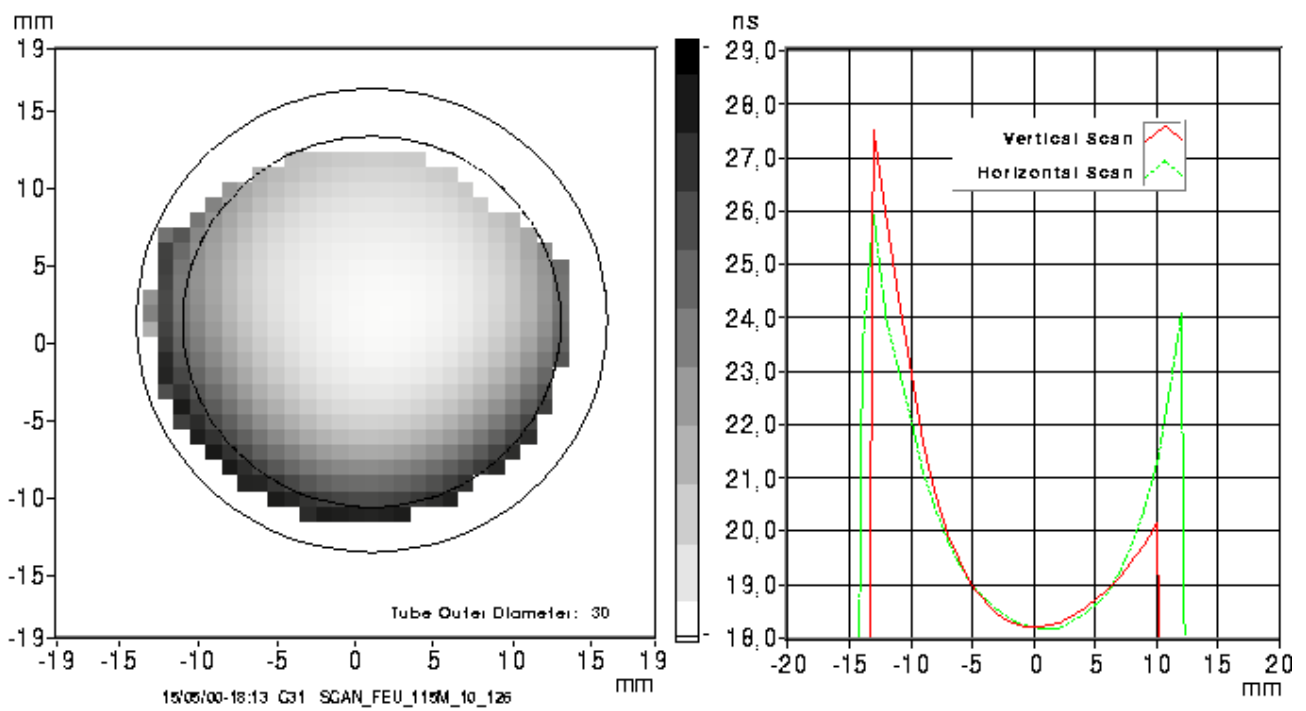


Figure 2-20

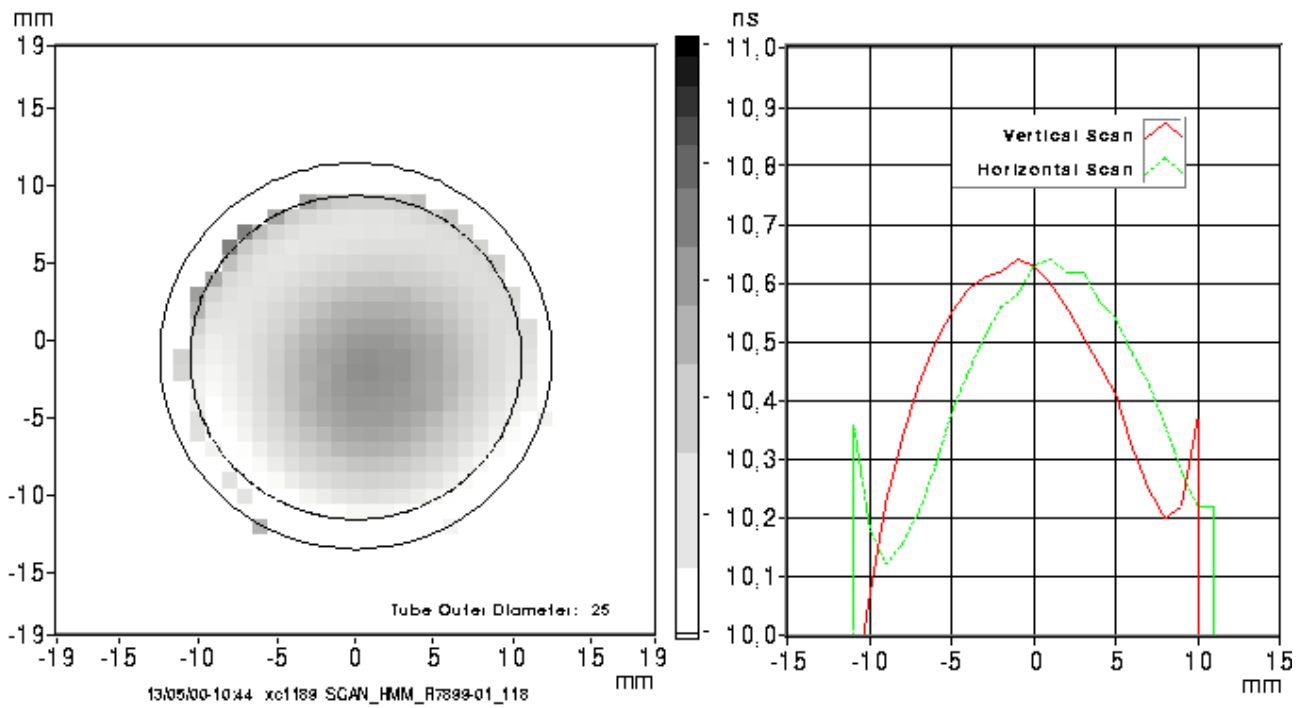


Figure 2-21

3 Magnetic shielding study

3.1 Magnetic measurement set-up

The set-up consists of two water cooled Helmholtz coils producing a field up to 600 Gauss. The size of the coils and the distance between them are large enough (Fig. 3-1) so that in a central region, corresponding to a cubic volume of $20 \times 20 \times 20 \text{ cm}^3$, the field is uniform within 10% (Fig. 3-2)

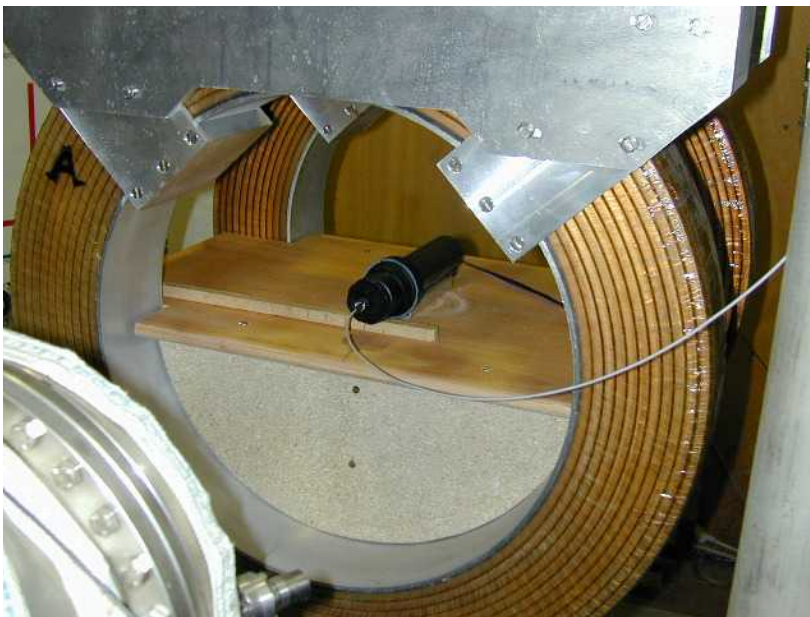


Figure 3-2 View of the Helmholtz coils.

3.2 Results for one shielding tube

As a shielding, we used a commercially available heating tube ($\phi = 42\text{mm}$) well matched to the PMT diameter. The 2.5-mm thick tube was long enough to give the possibility of sliding the PMT inside to study both the anode and the photocathode sensitivity to magnetic field. A mu-metal sheet, 0.8 mm thick, was wrapped around the PMT to minimise magnetic field effect. The study has been done for FEU115M-10 and Hamamatsu R5800. The Hamamatsu R7899 which was a development version, equipped with a socket of too big diameter, could not be used for this test.

A light pulse was produced by a fast led inside a light tight plastic box, attached to the iron tube. The PMT signal amplitude was measured with a digital oscilloscope. The amplitude variation ratio in percent is plotted (Fig.3-3, 3-4, 3-5) for four positions of the photocathode relative to the tube end as function of the nominal field without shielding. Already at 1cm, the shielding is effective for transverse field up to 300 Gauss. At a distance of 4 cm inside shielding, the effect of an axial field is tolerable up to 100 gauss.

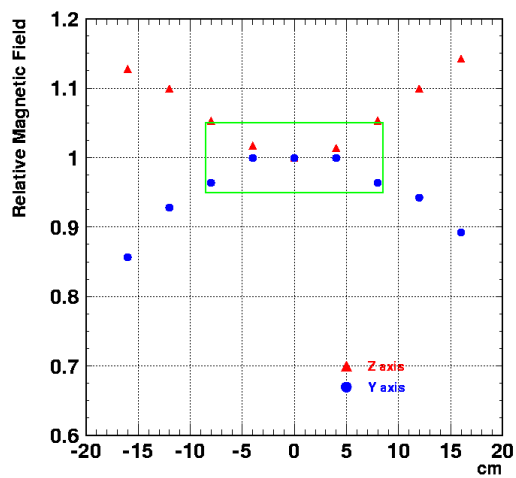


Figure 3-3 Field along Z and Y axis

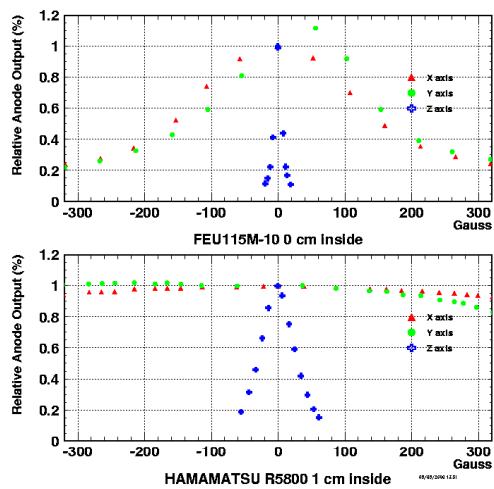


Figure 3-4 Photocathode 0 cm and 1 cm inside shielding

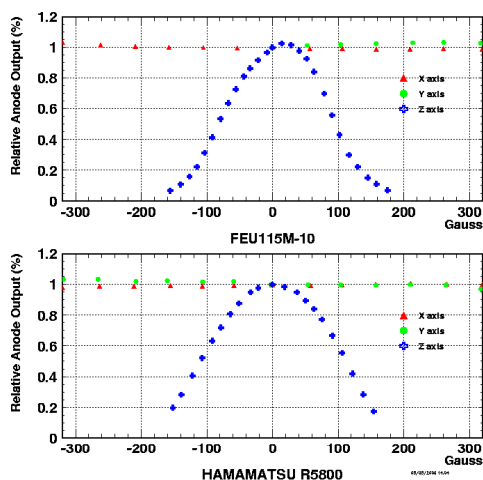


Figure 3-5 Photocathode 2 cm inside shielding

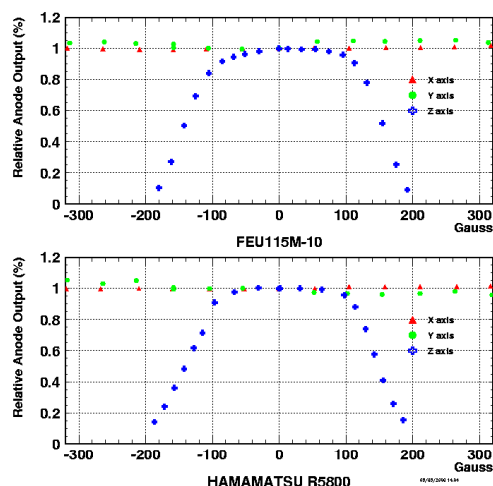


Figure 3-5 Photocathode 4 cm inside shielding

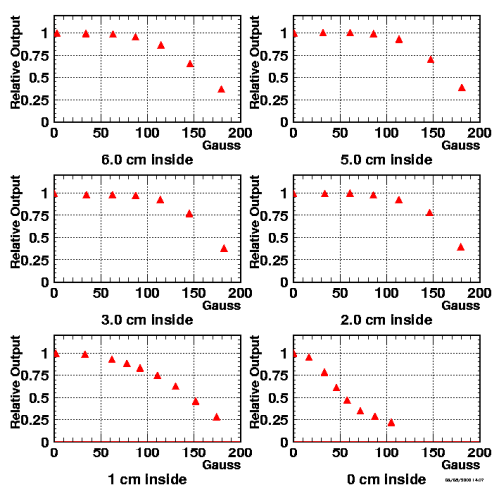


Figure.3-6 Output variations due to the anode position relative to tube end

Giving the R5800 PMT length, when the cathode is 4 cm inside the shielding, the anode is at 6 cm inside relative to the other end. The effect of the field on the anode has been measured starting from that position with the Hamamatsu R5800 only. One sees on Fig. 3-6 that no effect is visible up to 2 cm inside. As the end of the glass tube envelope exceeds precisely the anode position by 2 cm, the shielding does not need to be longer than the PMT thus its base could be located outside the shielding.

One should also notice in Fig. 3-6 that the position at 5 cm inside for the anode is slightly better than at 6 cm but no better than at 3 cm. The corresponding position for the cathode is 5 cm inside, but this position has not been measured.

3.3 Results with an array of nine shielding tubes

The preceding results overestimate the magnetic field effects. The shielding modifies the magnetic flux so the actual field at the tube level is increased. One sees (Fig 3-7) that the axial field measured along the z-axis at the entrance of the tube is more than twice the value without shielding. A measurement done with nine close packed tubes (Fig.3-8) which mimic the situation for the inner ECAL part, shows that the axial field at the end of the central tube is reduced to 100 Gauss. Consequently, the field immunity measured with only one shielding tube has been conservatively estimated.

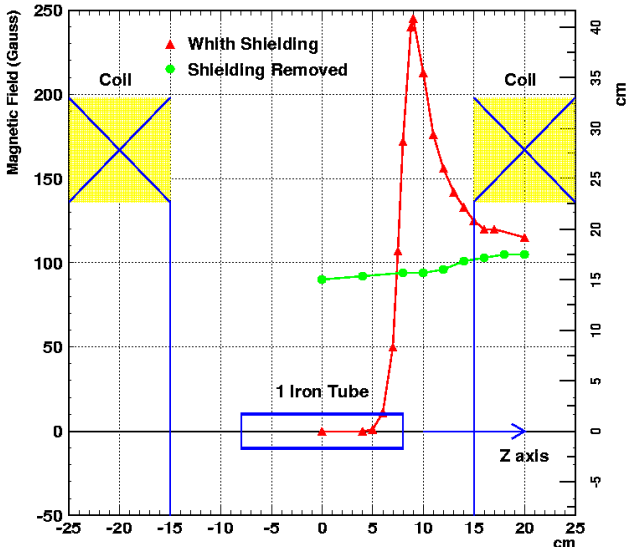


Figure 3-7 Axial field on the Z-axis with and without shielding tube.

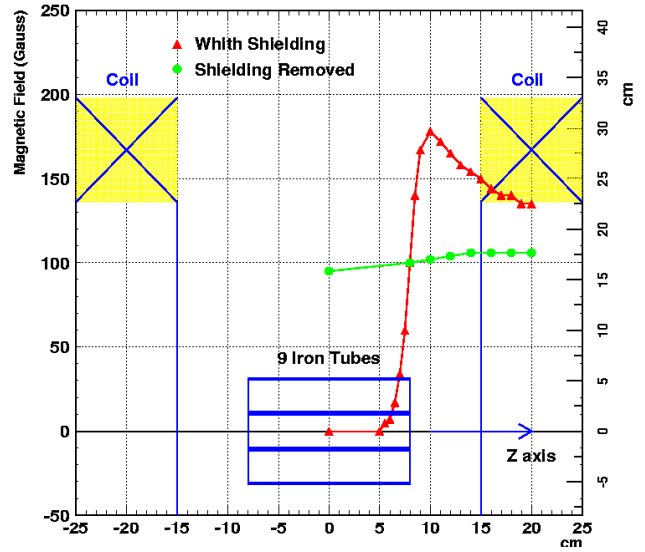


Figure 3-8 Axial field on the Z-axis with and without nine shielding tubes.

3.4 Conclusions for magnetic studies

Transverse field up to 300 Gauss and axial field up to 100 gauss can be tolerated providing that the shielding extends 4 cm beyond the photocathode.

4 Conclusions

Among the PMTs tested, three for the moment meet the need of the calorimeters. However, more studies are necessary to draw final conclusions. In particular, important characteristics like long term gain stability, recovery time, etc have yet to be considered.

5 References

[1] LHCb Collaboration, LHCb Technical Proposal, CERN/LHCC 98-4(1998)

[2] During the design period, we have had fruitful discussions with the IN2P3 Clermont-Ferrand ATLAS group. In particular, G. Montarou and M. Crouau helped us with their experience gained in testing the ATLAS Tile Calorimeter photomultipliers

[3] LHCb Calorimeter Technical Note LHCB 2000-39